

Superfluid Heat Conduction and the Cooling of Magnetized Neutron Stars

Deborah N. Aguilera,¹ Vincenzo Cirigliano,² José A. Pons,³ Sanjay Reddy,² and Rishi Sharma²

¹*Tandar Laboratory, Comisión Nacional de Energía Atómica,
Av. Gral. Paz 1499, 1650 San Martín, Buenos Aires, Argentina*

²*Theoretical Division, Los Alamos National Laboratory, Los Alamos, New Mexico 87545, USA*

³*Department of Applied Physics, University of Alicante,
Apartado de Correos 99, E-03080 Alicante, Spain*

We report on a new mechanism for heat conduction in the neutron star crust. We find that collective modes of superfluid neutron matter, called superfluid phonons (sPhs), can influence heat conduction in magnetized neutron stars. They can dominate the heat conduction transverse to magnetic field when the magnetic field $B \gtrsim 10^{13}$ G. At density $\rho \simeq 10^{12} - 10^{14}$ g/cm³ the conductivity due to sPhs is significantly larger than that due to lattice phonons and is comparable to electron conductivity when temperature $\simeq 10^8$ K. This new mode of heat conduction can limit the surface anisotropy in highly magnetized neutron stars. Cooling curves of magnetized neutron stars with and without superfluid heat conduction could show observationally discernible differences.

PACS numbers: 25.75.Nq, 26.60.+c, 97.60.Jd

Multiwavelength observations of thermal emission from the neutron star (NS) surface and explosive events such as superbursts in accreting NS and giant-flare in magnetars provide a real opportunity to probe the NS interior (see [1] and [2] for recent reviews). Theoretical models of these phenomena clearly underscore the importance of heat transport in the neutron star (NS) crust and have shown that it directly impacts observations. For example, nearby isolated compact X-ray sources that have also been detected in the optical band have a significant optical excess relative to the extrapolated X-ray blackbody emission (a factor 5 to 14) [3]. This optical excess can arise naturally if heat conduction in the NS crust is anisotropic due to the presence of a large magnetic field leading to an anisotropic surface temperature distribution [4, 5, 6]. In accreting NSs, the thermal conductivity directly affects the observed thermal relaxation time of the crust [7], and the superburst ignition depth and recurrence time-scale [8].

Typically, heat conduction is thought to arise due to the flow of relativistic electrons. Electrons are numerous, degenerate, and provide an efficient mode to transport heat. Conduction due to lattice phonons has been considered, but shown to be unimportant when the crust temperature $T \geq 10^6$ K [5, 9] and in NSs with low magnetic fields. In this letter we demonstrate that a new mechanism for heat transport arising due to the superfluid nature of the inner crust is important at high temperature and/or large magnetic fields. Here the heat is carried by the collective excitations of the neutron superfluid called superfluid phonons (sPhs).

This mode of conduction is especially relevant in NSs with moderate to high magnetic fields ($B \gtrsim 10^{13}$ G). In these cases, electron heat transport is very anisotropic because electrons can only move freely along magnetic field lines. Motion perpendicular to the field is restricted because the electron-cyclotron frequency is large compared to the inverse collision time. In contrast, sPhs, being electrically neutral excitations, are not directly af-

ected by magnetic fields. We find that sPh conduction is typically much larger than the electron conduction transverse to the field and this limits the degree of surface temperature anisotropy in magnetized NSs. In NSs with low magnetic fields, sPh conduction can still be relevant when the temperature is in the range $10^8 - 10^9$ K.

Free neutrons in the inner crust are known to form Cooper pairs and become superfluid at temperatures below the critical temperature $T_c \approx 10^{10}$ K. The superfluid ground state spontaneously breaks baryon-number symmetry and gives rise to a new massless Goldstone mode - the superfluid phonon (sPh). At long wavelengths, these phonons have a linear dispersion relation $\omega = v_s q$, where $v_s \simeq k_{\text{Fn}}/\sqrt{3}M$, M is the mass of the neutron and k_{Fn} is the neutron Fermi momentum. The thermal conductivity of a weakly interacting gas of sPhs can be computed from kinetic theory and is given by

$$\kappa_{\text{sPh}} = \frac{1}{3} C_V v_s \lambda_{\text{sPh}} \quad (1)$$

where $C_V = 2\pi^2 T^3/(15 v_s^3)$ is the specific heat of the phonon gas and λ_{sPh} is the typical mean free path of a thermal sPh. We can rewrite Eq. 1 using fiducial values of the temperature and the phonon velocity as

$$\kappa_{\text{sPh}} = 1.5 \times 10^{22} \left(\frac{T}{10^8 \text{ K}} \right)^3 \left(\frac{0.1}{v_s} \right)^2 \left(\frac{\lambda_{\text{sPh}}}{\text{cm}} \right) \frac{\text{erg}}{\text{cm s K}}. \quad (2)$$

This is to be compared with the thermal conductivity of electrons in the inner crust which is approximately 10^{18} erg cm⁻¹ s⁻¹ K⁻¹ when $T = 10^8$ K [10]. In the presence of large magnetic fields electron conduction in the direction perpendicular to the field can be several orders of magnitude smaller. Although sPhs are less numerous than the electrons they have large mean free paths because they interact weakly at long-wavelengths. In what follows we will estimate λ_{sPh} and its temperature dependence.

The low energy degrees of freedom in the inner crust are lattice phonons (lPhs), electrons, and sPhs. At

long-wavelengths, the excitations of the ion-lattice with mean number density n_I , mass number A and charge Z , are the longitudinal and transverse IPhs with velocities $c_s = \omega_P/q_{\text{TFe}}$ and $c_t \simeq 0.7 \omega_P/q_{\text{BZ}}$, respectively [11]. Here $\omega_P = \sqrt{4\pi e^2 Z^2 n_I / (AM)}$ is the ion-plasma frequency, $q_{\text{TFe}} = \sqrt{4e^2/\pi} p_{\text{Fe}}$ is the inverse Thomas-Fermi screening length of the electrons, p_{Fe} is the electron Fermi momentum, $q_{\text{BZ}} = (4.5\pi)^{1/3} a_i^{-1}$ and a_i is the inter-ion distance. The electrons are characterized by their Fermi momentum $p_{\text{Fe}} = (3\pi^2 Z n_I)^{1/3} \gg m_e \gg T$ and form a highly degenerate, relativistic Fermi gas. As mentioned earlier, the superfluid phonons (sPhs) are collective excitations of the neutron superfluid and their interactions are weak at low temperature. Their scattering cross section is parametrically suppressed by the factor T^8/μ_n^8 where $\mu_n = k_{\text{Fn}}^2/2M$ is the neutron chemical potential [12]. We note that when $T \simeq T_c$, sPhs are strongly damped as they can easily decay into neutron particle-hole excitations. However, since the crust cools to $T \ll T_c$ within several hours of the birth of the NS, this processes is exponentially suppressed by the factor $\exp(-2T_c/T)$ and the mean free path of sPhs is limited only by their interaction with IPhs, electrons and impurities.

The relevant processes are illustrated in Fig. 1: (i) Rayleigh scattering of phonons due to interactions with (compositional) impurities in the solid lattice [13]; (ii) absorption of sPhs due to their mixing with the longitudinal lattice phonons which are absorbed efficiently by electrons; and (iii) the decay of a sPh into two lattice phonons (IPhs).

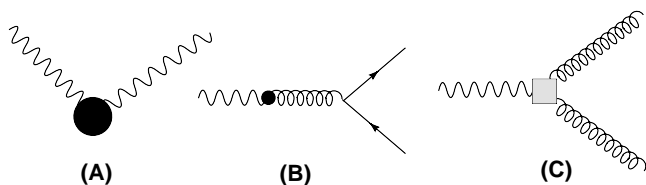


FIG. 1: Phonon scattering processes: (A) Rayleigh scattering; (B) phonon absorption by electrons; and (C) decay of sPhs into lattice phonons. The wavy-line is the sPh, the curly-line is the IPh, and the solid line are electrons, respectively.

At long-wavelength, the cross section for Rayleigh scattering of phonons by impurities is

$$\sigma_{\text{R}} = \pi r_0^2 \frac{(q r_0)^4}{1 + (q r_0)^4}, \quad (3)$$

where q is the phonon momentum and r_0 is an intrinsic strong-interaction length-scale related to the scattering length of the neutron-impurity system. This depends on the impurity composition and is expected to be about 10 fm. At low temperature, when $q r_0 \ll 1$, the mean free path of sPhs with thermal energy $\omega_{\text{th}} = 3T$ is

$$\lambda_{\text{Ray}} = (n_{\text{Im}} \sigma_{\text{R}})^{-1} = \frac{v_s^4}{81 n_{\text{Im}} \pi r_0^6 T^4}, \quad (4)$$

where $n_{\text{Im}} = 3/(4\pi d^3)$ is the impurity number density and d is the inter-impurity distance. Using fiducial values we can rewrite Eq. 4 as

$$\lambda_{\text{Ray}} = 450 \left(\frac{v_s}{0.1}\right)^4 \left(\frac{x}{10}\right)^3 \left(\frac{10 \text{ fm}}{r_0}\right)^3 T_7^{-4} \text{ cm} \quad (5)$$

where $x = d/r_0$ is the diluteness parameter for the impurities and T_7 is the temperature in 10^7 K.

We now show that inelastic processes such as sPh absorption by electrons and decay to IPhs shown in Fig. 1 (B) and (C) are more relevant. To study these processes we need a low-energy effective theory which couples the sPhs and IPhs. On general grounds, this effective theory can only contain derivative terms and at low temperature it is sufficient to retain the leading terms. The leading order Lagrangian that describes these interactions is of the form

$$\begin{aligned} \mathcal{L}_{\text{eff}} = & g_{\text{mix}} \partial_0 \phi \partial_i \xi^i + \frac{g_{\text{mix}}}{\Lambda^2} \partial_0 \phi \partial_i \xi_i \partial_j \xi_j \\ & + \frac{g_{\text{mix}}}{\Lambda_t^2} \partial_0 \phi \partial_i \xi_j \partial_i \xi_j + \dots \end{aligned} \quad (6)$$

where ϕ and $\xi_{i=1\dots 3}$ are the sPh and IPh (canonically normalized) fields, respectively. The first term describes the mixing between longitudinal IPhs and sPhs, and the second and third terms describe the process for the decay of a sPh into two longitudinal or transverse IPhs, respectively.

The coefficients of this effective theory are determined by computing the coupling between neutrons and lattice phonons in a manner similar to the calculation of the electron-phonon coupling in condensed matter physics [14]. We begin with the fundamental short-range interaction between neutrons and ions given by

$$\mathcal{H}_{\text{nI}} = \int d^3x d^3x' \Psi_I^\dagger(x) \Psi_I(x) V(x-x') \psi_n^\dagger(x) \psi_n(x)$$

where $V(x-x') = 2\pi a_{\text{nI}} \delta^3(x-x')/M$, is the neutron-ion low-energy potential and a_{nI} is the neutron-ion scattering length. By expanding the ion and neutron density fluctuations in terms of their collective modes we obtain

$$g_{\text{mix}} = 2 a_{\text{nI}} \sqrt{\frac{n_I k_{\text{Fn}}}{A M^2}}, \quad \Lambda^2 = \sqrt{n_I A M}, \quad (7)$$

respectively. For typical conditions in the NS crust $g_{\text{mix}} \simeq 10^{-3}$ and $\Lambda \simeq 50$ MeV. The specific details of this calculation and possible quantum corrections to the sPh-IPh interaction will be reported elsewhere [15]. Here we employ these results to estimate λ_{sPh} .

Mixing between sPhs and IPhs will damp sPh propagation because IPhs are strongly damped due to their interaction with electrons. To leading order in the small mixing parameter g_{mix} , the mean free path of sPhs with energy ω is given by

$$\lambda_{\text{abs}}(\omega) = \frac{v_s^2}{g_{\text{mix}}^2} \frac{1 + (1 - \alpha^2)^2 (\omega \tau_{\text{IPh}})^2}{\alpha (\omega \tau_{\text{IPh}})^2} \lambda_{\text{IPh}}(\omega), \quad (8)$$

where $\alpha = c_s/v_s$, and λ_{IPh} and $\tau_{\text{IPh}} = \lambda_{\text{IPh}}/c_s$ are the mean free path and lifetime of the IPh, respectively. At low temperature, where the Umklapp processes are frozen, we can estimate λ_{IPh} by assuming that the IPhs decay primarily by producing particle-hole excitations (normal processes) in the degenerate electron gas. We find that

$$\lambda_{\text{IPh-N}}(\omega) = f_{\text{ep}}^2 \frac{2\pi c_s^2}{p_{\text{Fe}}^2 \omega} = \frac{2}{3\pi} \frac{Z}{c_s^2} \frac{p_{\text{Fe}}}{A M \omega} = \frac{2}{\pi \omega} \quad (9)$$

where $f_{\text{ep}} = Z\sqrt{n_{\text{I}}/AM}/c_s^2$ is related to the electron-phonon coupling constant [16].

When $T \gtrsim T_{\text{Um}} = Z^{1/3} e^2 \omega_P/3$, the Umklapp processes begin to dominate [17] and in this regime $\lambda_{\text{IPh-U}} \simeq 100 a_i \simeq 2000 \text{ fm}$ [9]. The corresponding sPh mean free path is in the range $10^{-3} - 10^{-6} \text{ cm}$. At intermediate temperature we employ a simple interpolation formula given by

$$\lambda_{\text{IPh}}^{-1} = f_u \lambda_{\text{IPh-U}}^{-1} + (1 - f_u) \lambda_{\text{IPh-N}}^{-1}, \quad (10)$$

where $f_u = \exp(-T_{\text{Um}}/T)$ [17].

Finally we estimate the mean free path due to the decay process shown in the Fig. 1 (C). When the sPh velocity is greater than the IPh velocity this decay is kinematically allowed. The amplitude for the sPh of momentum q to split into two longitudinal IPh of momentum q_1 and q_2 is given by

$$\mathcal{A} \simeq \frac{g_{\text{mix}}}{\Lambda^2} \omega q_1 q_2. \quad (11)$$

The corresponding mean free path for a thermal phonon with energy $\omega = 3T$ can be calculated and we find that

$$\lambda_{\text{decay}} \simeq \frac{863}{f(\alpha)} \left(\frac{10^{-6}}{g_{\text{mix}}^2} \right) \left(\frac{c_s}{0.01} \right)^7 \left(\frac{v_s}{0.1} \right) \Lambda_0^4 T_7^{-5} \text{ cm} \quad (12)$$

where $\Lambda_0 = \Lambda/50 \text{ MeV}$, $f(\alpha) = 1 - 2\alpha^2/3 + \alpha^4/5$, and $\alpha = c_s/v_s$. For the temperatures of relevance we find that $\lambda_{\text{abs}} \ll \lambda_{\text{decay}}$ and $\lambda_{\text{abs}} \ll \lambda_{\text{Ray}}$. Consequently, only the sPh absorption process with the mean free paths given by Eq. 8 is relevant.

In Fig. 2 we employ the above result (Eq. 8) for the sPh mean free path and compare the thermal conductivity due to electron, IPhs, and sPhs transport in a typical NS crust, at temperatures of 10^8 K and 10^7 K . We show the electron contribution parallel (e^{\parallel}) and perpendicular (e^{\perp}) to the magnetic field lines for $B = 10^{13} \text{ G}$ and $B = 10^{14} \text{ G}$, according to [18]. Heat conduction due to lattice vibrations is primarily carried by the transverse modes because of their larger number density and we use the results from [9]. We can see that, above the neutron drip point, where a significant number of superfluid neutrons coexist with the electrons and the lattice, heat conduction due to sPh (red dot-dashed curve) is relevant, and is always significantly more efficient than conduction due to IPhs. The sPh conductivity decreases with depth and reaches a minimum when the velocity of the sPh becomes equal the longitudinal speed of sound due to the

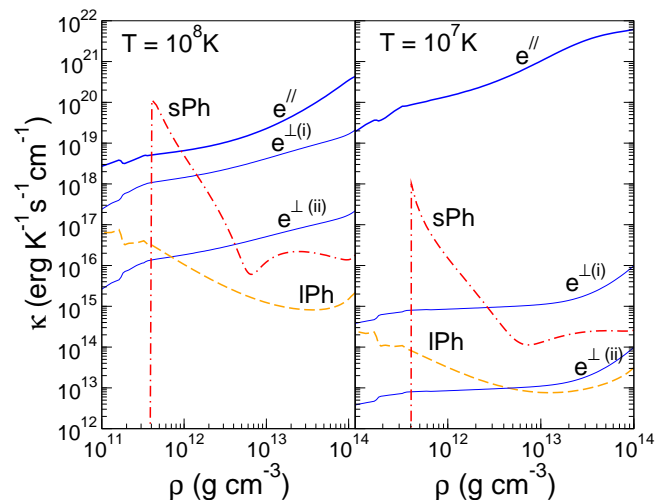


FIG. 2: Thermal conductivity in a NS crust for $T = 10^8 \text{ K}$ (left) and $T = 10^7 \text{ K}$ (right). The dot-dashed (red) curve shows the contribution due to sPhs. The thick (thin) solid lines show the electron conductivity in the direction longitudinal (perpendicular) to the magnetic field lines for $B = 10^{13} \text{ G}$ (i) and $B = 10^{14} \text{ G}$ (ii). The dashed lines (yellow) is the IPh contribution.

resonant mixing. Near neutron drip, where $v_s \ll c_s$ sPhs can even dominate over electron conductivity along the field. In the direction transverse to magnetic field the sPh conduction is shown to be relevant over much of the inner crust for fields $B \geq 10^{14} \text{ G}$.

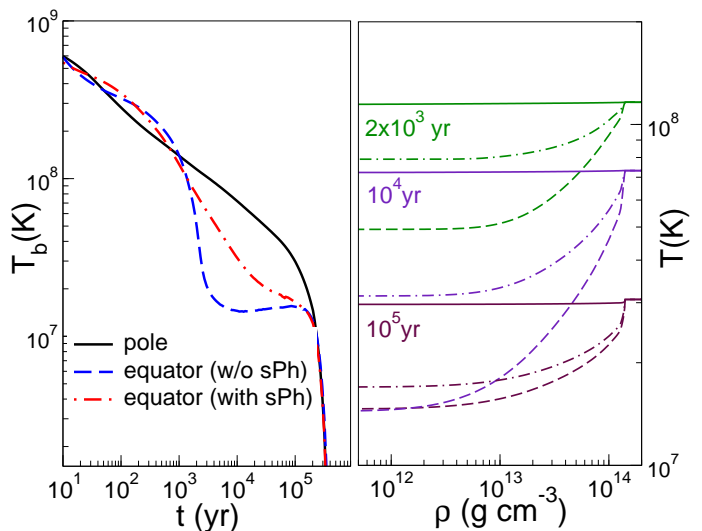


FIG. 3: Cooling curves of magnetized NS with and without considering sPhs. Left panel: T_b at the neutron drip point vs. age. Right panel: T vs. density for fixed times. The polar temperature (solid lines) is not affected, but the temperatures at the equator with sPhs (dash-dotted lines) and without sPhs (dashes) differ significantly.

To assess how this new mode of heat conduction might affect observable aspects of NS thermal evolution we have performed magnetar cooling simulations with and without including sPh conduction. Details regarding the simulation and the input physics are described in earlier work [19]. The new ingredients here are the sPh contribution to the thermal conductivity and the use of an updated 1S_0 neutron superfluid gap obtained from Quantum Monte Carlo simulations [20]. The cooling curves and temperature profiles for a NS model (Model A from Ref. [19]) with a poloidal, crustal magnetic field of strength $B = 5 \times 10^{13}$ G at the magnetic pole, are shown in Fig. 3. Temperatures at the magnetic equator are shown as dashed lines for the model without sPhs and as dashed-dotted lines for the model with sPhs. The temperature at the pole is shown by solid lines and there is no significant difference between the two cases. The left panel shows T_b , the temperatures at the neutron drip point ($\rho \approx 3 \times 10^{11}$ g cm $^{-3}$), as a function of the NS age, t . In the right panel we show the temperature profiles in the NS crust as a function of density, for three fixed times $t = 2 \times 10^3, 10^4, 10^5$ yr. The effect of sPhs is important, specially in the inner crust when $T \approx 10^8$ K. In the right panel one can see that sPhs partially reduce the otherwise strong temperature gradient generated along the inner crust. As a consequence, the temperature anisotropy in the inner crust is limited by sPh conduction. We note, however, that an anisotropy generated in the outer layers at density below neutron drip cannot be suppressed by sPhs.

Finally, we remark that even the phonon conductivity can be anisotropic. Large magnetic fields will induce an anisotropy in the electron response because of the gap in the electron excitation spectrum due to Landau quanti-

zation. When this gap is much larger than the temperature, phonons propagating transverse to the magnetic field cannot excite single electron-hole states and this is likely to greatly enhance both the lPh and sPh conductivity transverse to the field. Rotation will create superfluid vortices that will preferentially scatter sPhs propagating perpendicular to the rotation axis. Both these effects warrant further investigation.

Our estimate for the sPh conductivity, based on Eq. 1, can be improved by replacing the typical mean free path by an appropriate thermal average, and by accounting for composition and nuclear structure dependence of the neutron-nucleus scattering potential for neutron-rich nuclei in the crust. Nonetheless, our study clearly demonstrates that sPhs are important for heat conduction and are primarily damped through their mixing with the longitudinal lattice phonons. The sPh contribution is significantly larger than lPhs and the magnitude of the temperature anisotropy generated at deep crustal layers is likely to be limited by superfluid heat conduction. If future observations allow us to establish a clear correlation between surface temperature distribution, magnetic field orientation and age, we may be able to probe the superfluid nature of the NS inner crust.

Acknowledgments: We thank the organizers and participants of the INT workshop on neutron star crust, especially, C. Horowitz and A. Cumming, for stimulating discussions. We also thank T. Bhattacharya, A. Chugunov, J. A. Miralles and D. Yakovlev for many interesting comments. This research was supported by the Dept. of Energy under contract DE-AC52-06NA25396, by the Spanish MEC grant AYA 2004-08067-C03-02 and by CONICET, Argentina. The work of SR was funded in part by the LDRD program at LANL under grant number 20080130DR.

-
- [1] D. G. Yakovlev and C. J. Pethick, *ARA&A* **42**, 169 (2004), arXiv:astro-ph/0402143.
 - [2] D. Page and S. Reddy, *Ann. Rev. Nucl. Part. Sci.* **56**, 327 (2006), astro-ph/0608360.
 - [3] F. Haberl, *Ap&SS* **308**, 181 (2007), arXiv:astro-ph/0609066.
 - [4] U. Geppert, M. Küker, and D. Page, *A&A* **426**, 267 (2004), arXiv:astro-ph/0403441.
 - [5] J. F. Perez-Azorin, J. A. Miralles, and J. A. Pons, *Astron. Astrophys.* **451**, 1009 (2006), astro-ph/0510684.
 - [6] U. Geppert, M. Küker, and D. Page, *A&A* **457**, 937 (2006), arXiv:astro-ph/0512530.
 - [7] P. S. Shternin, D. G. Yakovlev, P. Haensel, and A. Y. Potekhin, *MNRAS* **382**, L43 (2007), arXiv:0708.0086.
 - [8] E. F. Brown, L. Bildsten, and R. E. Rutledge, *ApJ* **504**, L95+ (1998), arXiv:astro-ph/9807179.
 - [9] A. I. Chugunov and P. Haensel, *MNRAS* **381**, 1143 (2007), arXiv:0707.4614.
 - [10] P. S. Shternin and D. G. Yakovlev, *Phys. Rev. D* **74**, 043004 (2006), arXiv:astro-ph/0608371.
 - [11] E. Flowers and N. Itoh, *ApJ* **206**, 218 (1976).
 - [12] D. T. Son and M. Wingate, *Annals Phys.* **321**, 197 (2006), cond-mat/0509786.
 - [13] G. Baym and C. Ebner, *Physical Review* **164**, 235 (1967).
 - [14] A. Fetter and J. Walecka, *Quantum Theory of Many-Particle Systems*, vol. 26 (McGraw-Hill Book Co., New York, 1971).
 - [15] V. Cirigliano, S. Reddy, and R. Sharma, in preparation (2008).
 - [16] J. M. Ziman, *Electrons and Phonons* (Oxford Univ. Press, Oxford, 1960).
 - [17] O. Y. Gnedin, D. G. Yakovlev, and A. Y. Potekhin, *MNRAS* **324**, 725 (2001), arXiv:astro-ph/0012306.
 - [18] A. Y. Potekhin, *A&A* **351**, 787 (1999), arXiv:astro-ph/9909100.
 - [19] D. N. Aguilera, J. A. Pons, and J. A. Miralles, *A&A* **486**, 255 (2008), arXiv:0710.0854.
 - [20] A. Gezerlis and J. Carlson, *Phys. Rev. C* **77**, 032801 (2008), arXiv:0711.3006.